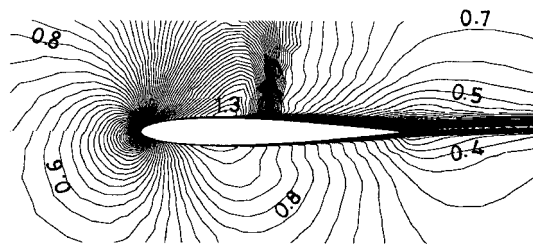


a) Streamline plot in laminar flow



b) Mach contours in turbulent flow

Fig. 6 Flow over an isolated NACA-0012 airfoil.

A C-type boundary-layer grid around a NACA-0012 airfoil has been generated up to a normal distance corresponding to $\Delta/C_h = 0.06$. The values of N and s are 20 and -4 , respectively. This boundary-layer mesh is coupled with unstructured and algebraic meshes as shown in Fig. 5. Figure 6a shows the streamlines in laminar flow with the conditions for freestream Mach number $M_\infty = 0.5$, Reynolds number based on chord $Re_{ch} = 5 \times 10^3$ and incidence $\alpha = 0$ deg, same as those used by Liu.⁴ The present results, including a small separation zone near the trailing edge, are in good agreement with Liu.⁴ Figure 6b shows the isentropic Mach-number contours for the turbulent compressible flow at $M_\infty = 0.754$, $Re_{ch} = 3.76 \times 10^6$, and $\alpha = 3.02$ deg. With the help of hyperbolic grid, the Baldwin-Lomax turbulence model has been implemented without any complex changes, such as those suggested by Turner and Jennions.⁵ The standard $k-\epsilon$ model is used in the unstructured and algebraic grid zones. This result is in good agreement with the predictions of Kallinderis.⁶

Conclusions

A hyperbolic grid-generation technique is proposed based on analytical geometric considerations. The main feature of the method is generation of orthogonal quadrilateral cells with controllable cell area. The grid generated by the proposed method is found to be convenient for accurate prediction of laminar and turbulent flow past arbitrary shaped bodies.

References

- Thompson, J. F., "Grid Generation Techniques in Computational Fluid Dynamics," *AIAA Journal*, Vol. 22, No. 11, 1984, pp. 1505–1523.
- Hoffman, K. A., and Chiang, S. T., "Grid Generation-Structured Grids," *Computational Fluid Dynamics for Engineers*, Vol. 1, Engineering Education Systems, Wichita, KS, 1993, pp. 344–411.
- Tai, C. H., Yin, S. L., and Sorg, C. Y., "A Novel Hyperbolic Grid Generation Procedure with Inherent Adaptive Dissipation," *Journal of Computational Physics*, Vol. 116, No. 1, 1995, pp. 173–179.
- Liu, F., "Numerical Calculation of Turbomachinery Cascade Flows," Ph.D. Dissertation, Dept. of Mechanical and Aerospace Engineering, Princeton Univ., Princeton, NJ, June 1991.
- Turner, M. G., and Jennions, I. K., "An Investigation of Turbulence Modelling in Transonic Fans Including a Novel Implementation of an Implicit $k-\epsilon$ Turbulence Model," *Journal of Turbomachinery*, Vol. 115, No. 2, 1993, pp. 249–307.
- Kallinderis, Y., "Algebraic Turbulence Modelling for Adaptive Unstructured Grids," *AIAA Journal*, Vol. 30, No. 3, 1992, pp. 631–639.

J. Kallinderis
Associate Editor

Mixing Enhancement in Compressible Base Flows via Generation of Streamwise Vorticity

C. J. Bourdon* and J. C. Dutton†

University of Illinois at Urbana-Champaign,
Urbana, Illinois 61801

Introduction

PREVIOUS studies employing flow visualization techniques and pitot pressure measurements^{1–3} have shown that asymmetries in the pressure field of the jets issuing from ideally expanded converging and ideally or overexpanded converging-diverging nozzles are caused by stationary streamwise vortices present in the flowfield. The origins of these vortices have been traced to imperfections in the nozzle surface. Krothapalli et al.³ assert that imperfections as small as $\frac{1}{12}$ th of the boundary-layer velocity deficit thickness are sufficient to trigger such behavior.

Stationary streamwise vortices such as these were shown to improve the mixing characteristics of axisymmetric jet flows⁴ by increasing the stream interface area and overall shear layer thickness. Therefore, these researchers found it beneficial to promote streamwise vorticity generation by inserting surface disturbances onto the nozzle lip. King et al.⁴ found that the most effective shape for generating streamwise vortices in a supersonic jet is an isosceles triangular tab, placed flush on the surface, with an apex angle of 25–30 deg. This study also found that increasing the tab thickness increased the shear layer thickness, although the benefit was relatively small when compared to that of the thinnest significant tab disturbance.

Extension of such a technique to base flows seems quite natural. If the streamwise vorticity generated from the tabs survives the base corner expansion fan, which has been shown⁵ to damp turbulence in the developing shear layer, it could significantly influence the turbulence structural organization in the near-wake region. Influencing the turbulent structure organization (and thus mixing between the freestream and core fluid) may substantially alter the base pressure and drag characteristics of a bluff object. This is the subject of the current Note.

Flow Facility and Equipment

The axisymmetric, supersonic flow facility in the University of Illinois Gas Dynamics Laboratory was employed in this study. The base model is supported by a 63.5-mm-diam sting, which extends through the supersonic converging-diverging nozzle. The freestream flow before separation from the base model is at a Mach number of 2.46, with a unit Reynolds number of $52 \times 10^6 \text{ m}^{-1}$, and typical stagnation conditions of $P_0 = 368 \text{ kPa}$ and $T_0 = 300 \text{ K}$. The turbulent boundary-layer thickness on the sting/afterbody just before separation has been measured to be 3.2 mm (Ref. 5). A schematic of the main features of the base region are given in Fig. 1.

The surface disturbances were formed in this study by application of pieces of adhesive shipping label to the surface of a blunt-based afterbody. As stated earlier, disturbances as small as $\frac{1}{12}$ th of the velocity deficit thickness have been found sufficient to produce asymmetries in overexpanded and ideally expanded jets.³ In our facility, this translates to a disturbance thickness of approximately 0.1 mm (Ref. 5), the approximate thickness of the shipping label material. The disturbance thickness was altered by applying multiple layers of the labeling material.

Received 11 March 2001; revision received 16 April 2001; accepted for publication 18 April 2001. Copyright © 2001 by C. J. Bourdon and J. C. Dutton. Published by the American Institute of Aeronautics and Astronautics, Inc., with permission.

*Graduate Research Assistant, Department of Mechanical and Industrial Engineering, Student Member AIAA.

†W. Grafton and Lillian B. Wilkins Professor, Department of Mechanical and Industrial Engineering, Associate Fellow AIAA.

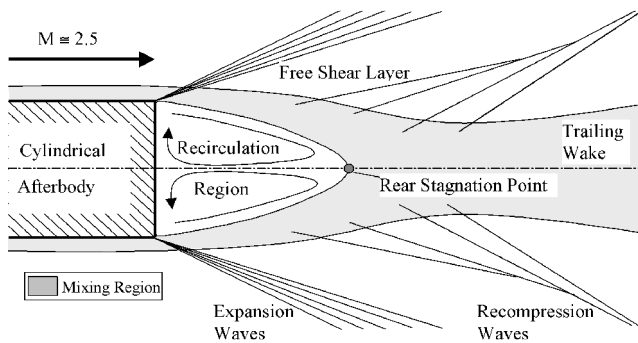


Fig. 1 Schematic of mean blunt-base flowfield.

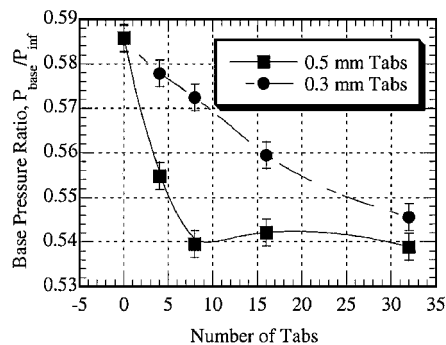


Fig. 2 Effect of delta-shaped tabs on the base pressure of a cylindrical afterbody.

For imaging data acquisition, a planar Rayleigh/Mie scattering technique was implemented in this study. Liquid ethanol is injected into carrier air approximately 1.5 m upstream of the facility plenum chamber. The ethanol quickly evaporates as it is carried into the plenum. As the ethanol and carrier air are accelerated supersonically, the rapid expansion causes the vapor to condense (at conditions that correspond to a Mach number of approximately unity⁶) into a fine mist. A thin laser sheet, generated by a ND:YAG laser illuminates the mist, and a 14-bit, back-illuminated, unintensified Photometrics charge-coupled device camera is used to image the illuminated droplets.

Results and Discussion

In accordance with previous work,⁴ the tab geometry has been chosen to have an apex angle of 30 deg, a width of 6.2 mm ($\frac{1}{32}$ of the base radius), and a thickness of 0.1 mm or greater. In preliminary results, tab thicknesses of 0.3 mm or greater were found to produce more profound effects on the shear layer, while not creating significant flow blockage, than the 0.1-mm-thick tabs. Therefore, all further work reported here is for tab thicknesses of 0.3 and 0.5 mm.

Figure 2 presents the effect that uniformly spaced tabs of 0.3 and 0.5 mm thicknesses have on the afterbody base pressure as a function of the number of tabs. The measurement uncertainty is indicated by vertical bars and is approximately 5% of the measured value. The presence of the tab disturbances does lead to decreased pressure on the base (increased entrainment from the separated region), as expected. For the 0.5-mm-thick tabs, the base pressure is shown to decrease steeply with the addition of more tabs. For geometries containing more than eight tabs of 0.5 mm thickness, the effect of additional tabs is diminished, and the base pressure asymptotes to a value approximately 10% lower than that for no disturbances. The base pressure asymptote approached with increasing tab number appears to be similar for the 0.3-mm tabs as for the 0.5-mm tabs, although the rate of decrease is smaller.

Based on the base pressure results shown in Fig. 2, a detailed imaging analysis of the eight-tab case was conducted. Instantaneous and average images were acquired in both the side- and end-view orientations (Figs. 3 and 4) for both the 0.3- and 0.5-mm-thickness cases. The images obtained for the 0.3-mm-thick tab case are qualitatively similar to the 0.5-mm tab case, and so they are not presented for the sake of brevity.

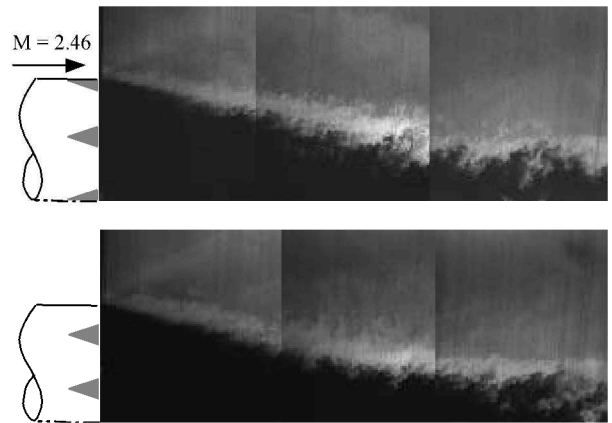


Fig. 3 Instantaneous global composite images of near-wake flowfield for plane centered on (top) and between (bottom) tabs (0.5 mm thick).

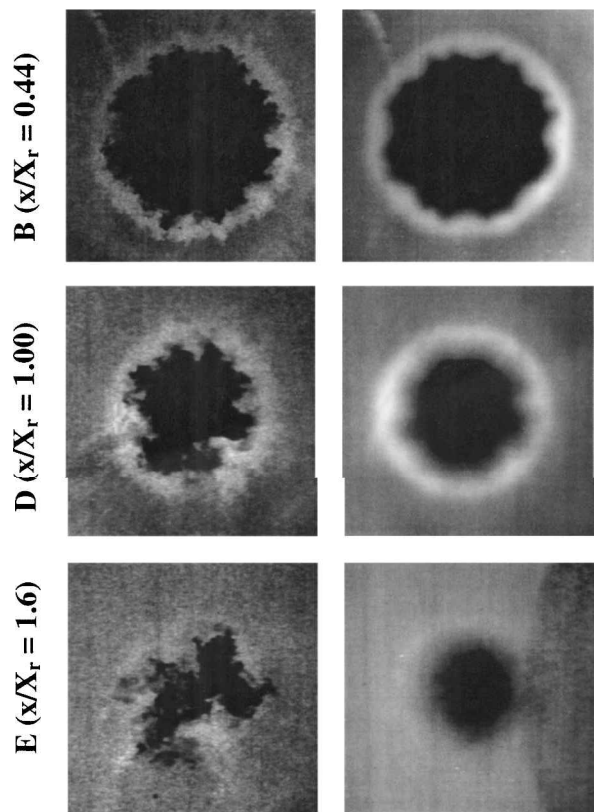


Fig. 4 Instantaneous (left) and average (right) end-view images from the free shear layer (B, top), mean reattachment (D, center), and trailing wake (E, bottom) regions (0.5-mm-thick tabs).

Side-view global composite images have been acquired both along the center axis of the tab (Fig. 3, top) and in the plane between tabs (Fig. 3, bottom). The most important features visible in these composite images are the turbulent structures that exist along the interface between the outer freestream and recirculating flows. The character of these structures is significantly different than what is seen in the no-tab case.⁷ The structures appear to be more evenly spaced (or more organized) than for the blunt-base case before the mean reattachment point (just to the right of the center of the image). The blunt-base study⁷ demonstrated some evidence of regular turbulent structure spacing in the side view after the mean reattachment point, but not before. Also note that there are both more structures visible and that the structures are apparently larger along the tab axis (Fig. 3, top) than in the plane between tabs (Fig. 3, bottom).

The reason for the latter differences seen in the side views is apparent when examining the mean and instantaneous end-view images presented in Fig. 4. The large streamwise-oriented structures are aligned along the base corners of the delta-tab disturbances. The

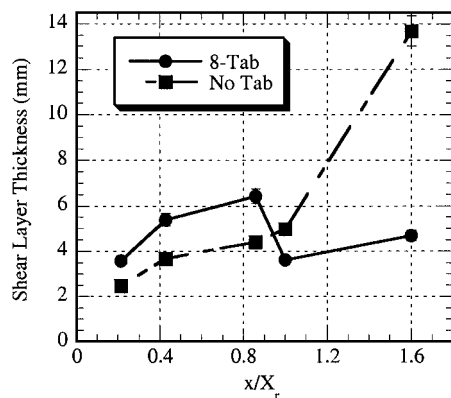


Fig. 5 Average shear layer thickness of 0.5-mm-thick, eight-tab case.

mean images (right-hand side of Fig. 4) show that w-shaped disturbances persist behind the tab positions along the interface all of the way to reattachment (Fig. 4D). King et al.⁴ suggest that this w-shaped feature is caused by the presence of a counter-rotating streamwise vortex pair. If this suggestion is indeed correct, then the large-scale turbulence, which is randomly oriented in the absence of tabs, has been organized into streamwise vortices due to the presence of the tabs in this base flow.

In the trailing wake (Fig. 4E), the mean images show no lingering organized disturbances in the flowfield, and the mean shear layer appears to be circular and symmetric, as in the no-tab case. This suggests that the reattachment process destabilizes the organization of the streamwise vortices, because of the influence of extra strain rates, such as lateral streamline convergence, concave streamline curvature, adverse pressure gradients, and axisymmetric confinement. Evidence of such phenomena in blunt-based afterbody flows,⁷ obtained via spatial correlation analysis, also suggests that this occurs. The current images are among the first to demonstrate visually that the reattachment process randomizes the large-scale turbulent structure organization in compressible base flows.

The average shear layer thickness at five measurement locations, measured from the average end-view images (Fig. 4, right), is presented in Fig. 5. The experimental uncertainty of these measurements is approximately 5%, as indicated by the vertical bars in the figure. These measurements show that, near the base, the shear layer growth rate is significantly larger for the eight-tab case than the no-tab case. This indicates that entrainment and mixing near the base are enhanced by the streamwise vorticity generated by the delta-shaped disturbances. This is, of course, consistent with the lower base pressures measured for the tabbed cases compared to the no-tab case (Fig. 2).

The last feature of interest in Fig. 5 is the large decrease in shear layer thickness for the eight-tab case at the mean reattachment point, $x/X_r = 1.0$. As indicated in the average images (Fig. 4, right), the organization of the streamwise vortices appears to diminish significantly at reattachment and disappears completely in the near wake. The recompression and reattachment processes thus significantly weaken the organized structures present within this flow, being predominantly associated with the streamwise vortices formed from the delta-shaped tabs.

Conclusions

This work demonstrates the effects that adding streamwise vorticity to the boundary layer of an axisymmetric afterbody, through the use of delta-shaped tabs mounted on the afterbody, has on the development of the near-wake region. The streamwise vorticity generated by the tabs persists through the base corner expansion and into the near wake, increasing mixing and base drag. The reattachment process destabilizes the streamwise structures, and there is no trace of these structures in the average end-view images of the developing wake beyond reattachment.

Acknowledgments

Funding for this research is provided through the U.S. Army Research Office, Grant DAAG55-97-1-0122, with Thomas L. Doligalski as Technical Monitor.

References

- ¹Zapryagaev, V. I., and Solotchin, A. V., "Development of Streamwise Vortices in the Initial Section of a Supersonic Non-Isobaric Jet in the Presence of Microroughness of the Inner Nozzle Surface," *Fluid Dynamics*, Vol. 32, No. 3, 1997, pp. 465–469.
- ²Zapryagaev, V. I., and Solotchin, A. V., "An Experimental Investigation of the Nozzle Roughness Effect on Streamwise Vortices in a Supersonic Jet," *Journal of Applied Mechanics and Technical Physics*, Vol. 38, No. 1, 1997, pp. 78–86.
- ³Krothapalli, A., Strykowski, P. J., and King, C. J., "Origin of Streamwise Vortices in Supersonic Jets," *AIAA Journal*, Vol. 36, No. 5, 1998, pp. 869–872.
- ⁴King, C. J., Krothapalli, A., and Strykowski, P. J., "Streamwise Vorticity Generation in Supersonic Jets with Minimal Thrust Loss," AIAA Paper 94-0661, 1994.
- ⁵Herrin, J. L., and Dutton, J. C., "Supersonic Base Flow Experiments in the Near Wake of a Cylindrical Afterbody," *AIAA Journal*, Vol. 32, No. 1, 1994, pp. 77–83.
- ⁶Smith, K. M., "The Role of Large Structures in Compressible Reattaching Shear Flows," Ph.D. Dissertation, Dept. of Mechanical and Industrial Engineering, Univ. of Illinois, Urbana, IL, 1996.
- ⁷Bourdon, C. J., and Dutton, J. C., "Planar Visualizations of Large-Scale Turbulent Structures in Axisymmetric Supersonic Separated Flows," *Physics of Fluids*, Vol. 11, No. 1, 1999, pp. 201–213.

J. P. Gore
Associate Editor